Computational study of the energetics of charge and cation mixing in $U_{1-x}Ce_xO_2$

B. E. Hanken

Department of Chemical Engineering and Materials Science, University of California, Davis, California 95616, USA

C. R. Stanek

Materials Science & Technology Division, Los Alamos National Laboratory, Los Alamos, New Mexico 87545, USA

N. Grønbech-Jensen

Department of Applied Science, University of California, Davis, California 95616, USA

M. Asta

Department of Materials Science and Engineering, University of California, Berkeley, California 94720, USA and Department of Chemical Engineering and Materials Science, University of California, Davis, California 95616, USA

The formalism of electronic density-functional theory (DFT), with Hubbard-U corrections (DFT + U), is employed in a computational study of the energetics of fluorite-structured $U_{1-x}Ce_xO_2$ mixtures. The computational approach makes use of a procedure which facilitates convergence of the calculations to multiple self-consistent DFT + U solutions for a given cation arrangement, corresponding to different charge states for the U and Ce ions in several prototypical cation arrangements. Results indicate a significant dependence of the structural and energetic properties on the nature of both charge and cation ordering. With the effective Hubbard-U parameters that reproduce well the measured oxidation-reduction energies for urania and ceria, we find that charge transfer between U^{4+} and Ce^{4+} ions, leading to the formation of U^{5+} and Ce^{3+}, gives rise to an increase in the mixing energy in the range of 4–14 kJ/mol of the formula unit, depending on the nature of the cation ordering. The results suggest that although charge transfer between uranium and cerium ions is disfavored energetically, it is likely to be entropically stabilized at the high temperatures relevant to the processing and service of urania-based solid solutions.

PACS number(s): 82.60.Lf, 71.15.Mb, 82.60.Cx

I. INTRODUCTION

The thermophysical properties of urania-ceria mixtures have been investigated for more than three decades[1–13] due to the relevance of these materials to the understanding of nuclear fuel behavior. Cerium is a fission product that is highly soluble in urania (UO_2) (Ref. 1), and its effects on phase stability, thermal conductivity, and ionic diffusion are thus relevant to the performance of oxide fuels, particularly at high burnup. Further, the urania-ceria system has been widely investigated as a surrogate for urania-plutonia mixed-oxide (MOX) fuels, owing to the similar oxidation states and ionic radii for Ce and Pu ions.

For oxygen (O) to metal (M) stoichiometries of O/M = 2, the U-Ce-O phase diagram has been well characterized and features a continuous series of solid solutions connecting the UO_2 and CeO_2 compounds.[1–3] Over the range of temperatures where these solid solutions can be equilibrated, ($U_{1-x}Ce_x$)O_2 mixtures have been observed to form homogeneously disordered solid solutions with the cubic fluorite crystal structure, and no evidence has been reported for the formation of ordered superstructures. Single-phase fluorite solid solutions are also observed to be stable over a range of nonstoichiometric O/M ratios, although for cerium-rich compositions the phase field is characterized by a miscibility gap separating mixtures with O/M ratios near to and significantly lower than 2 (Refs. 1–3). In addition to the extensive studies of phase equilibria, a variety of thermophysical properties have been measured for urania-ceria mixtures. These properties include oxygen partial molar free energies and enthalpies,[4] lattice parameters,[5]

bond lengths,[6] heat capacities,[7,8] magnetic properties,[9–11] and electronic structure.[12,13] While many of the properties of urania-ceria are relatively well characterized, there are, at present, no published values of the mixing thermodynamic properties (enthalpy, entropy, and free energy) that the authors are aware of. Additionally, an important issue that remains incompletely understood is the existence of mixed cation valence states, originating from the charge transfer between U and Ce cations.

The ideal cation charge states in ($U_{1-x}Ce_x$)O_2 are 4+, and correspond to $5f^2$ and $4f^0$ electronic configurations for U^{4+} and Ce^{4+} ions, respectively. As reviewed in Refs. 9,12, it was first reported nearly a century ago that Ce-rich urania-ceria solid solutions form a deep blue color that stands in sharp contrast to the yellow and brown colors of pure CeO_2 and UO_2, respectively. As reviewed by Griffiths *et al.*, this deep blue color has been proposed to arise from the charge transfer between U and Ce cations, forming a solid solution composed of mixed charge states.[14] Specifically, Griffiths *et al.* proposed the following reaction:[14]

$$Ce^{4+}(4f^0) + U^{4+}(5f^2) \rightarrow Ce^{3+}(4f^1) + U^{5+}(5f^1). \quad (1)$$

The presence of multiple cation valence states is expected to have important consequences for the thermophysical properties of urania-ceria solid solutions. For example, it has been shown in battery materials[15] that the (electronic) configurational entropy associated with the arrangements of the differently charged cation species can have pronounced effects

on mixing thermodynamic properties and high-temperature phase equilibria.

Recent experimental studies have reached conflicting conclusions concerning the extent of the type of charge transfer reactions given by Eq. (1). In a series of papers reporting measurements of magnetic properties for a range of cerium compositions, Hinatsu and Fujino concluded that solid solutions with low cerium fraction exhibited some formation of Ce^{3+} and U^{5+}, while those of higher cerium fraction (>0.50) even form Ce^{3+} and U^{6+}.[9–11] In contrast to these conclusions, x-ray absorption near edge structure (XANES) measurements performed by Antonio *et al.* for a $(U_{0.33}Ce_{0.67})O_2$ solid solution were reported to show no evidence for the presence of Ce^{3+} or U^{5+} ions. In discussing their findings in relation to the results obtained by Hinatsu and Fujino, Antonio *et al.* hypothesized the anomalous magnetic susceptibility measured by these authors arises from oxygen $2p$ hybridization with cerium $4f$ orbitals, which would add a Pauli paramagnetic term not accounted for in the work by Hinatsu and Fujino. In a more recent study, Bera *et al.* performed x-ray photoelectron spectroscopy (XPS) measurements for urania-ceria solid solutions with a wide range of cation compositions and O/M ratios.[13] Based on their measurements it was concluded that a significant fraction of the U and Ce ions near the surface exist in the 5+ and 3+ charge states for nearly stoichiometric O/M ratios, and the concentration of cations with charge states other than 4+ was reported to be highly sensitive to changes in the O/M ratios. Unfortunately, the XANES results of Antonio *et al.* were not discussed by Bera *et al.*, and the origin of the conflicting conclusions reached in the two studies concerning the presence of mixed-charged cations in urania-ceria solid solutions remains unclear.

To gain further insight into charge mixing and its effects on thermodynamic properties of urania-ceria solid solutions, we undertake in this work an investigation of the energetics of $(U_{1-x}Ce_x)O_2$ solid solutions within the framework of electronic density-functional theory, including the Hubbard-U corrections required to accurately describe the insulating nature of the electronic structure of UO_2 (Ref. 16). Using values of the Hubbard-U parameters which reproduce well the energetics of relevant redox reactions in urania and ceria, we calculate the mixing energies of urania-ceria mixtures, considering a variety of prototypical cation arrangements, with both ideal and mixed-charge states. Based on the results of the DFT + U calculations we refine classical potential models for this system and use these potentials to investigate the enthalpy and entropy of mixing of disordered urania-ceria solid solutions. Details of the computational approaches are described in the next section, and relevant results from the DFT + U and classical-potential model calculations are then presented in Sec. III. The results are summarized and discussed in the context of the experimental observations described above in Sec. IV.

II. METHODS

To investigate the energetics of charge and cation mixing in the urania-ceria system, we consider a set of fluorite-based superstructures in which the cations are arranged in accor-

dance with several fcc-based prototypical ordered compounds. Cation arrangements in these structures are built from ordering waves along the ⟨100⟩, ⟨210⟩, and ⟨111⟩ "special-point" ordering directions,[21] and include the so-called "Lifshitz structures" for ordering on the fcc cation sublattice of the fluorite structure. All structures considered in this work have stoichiometric oxygen concentrations (i.e., the oxygen fluorite sublattice is fully occupied with no vacancy or interstitial oxygen atoms present). Experimentally, urania-ceria solid solutions are observed to be configurationally disordered on the cation sublattice. However, in the present work we consider only the ordered structures shown in Fig. 1 and listed in Table I in the DFT + U calculations. To model the energetics of disordered solid solutions, we show that pair-potential models closely match the DFT + U results, after adjusting a parameter giving the difference between the uranium and cerium fifth and fourth ionization potentials. These models are subsequently used in supercell calculations of random mixtures.

In our calculations we consider two types of ionic charge states. In the first, which we will refer to as "ideal charge states" (ICS), all cerium and uranium ions possess the 4+ charge state (see discussion below for the definition of the charge states based on the results of the electronic structure calculations). In the second, which we will refer to as "mixed charge states" (MCS), a fraction of the cerium and uranium ions are, respectively, reduced and oxidized to 3+ and 5+ charge states in a 1:1 ratio of Ce^{3+}:U^{5+} to preserve overall charge neutrality.
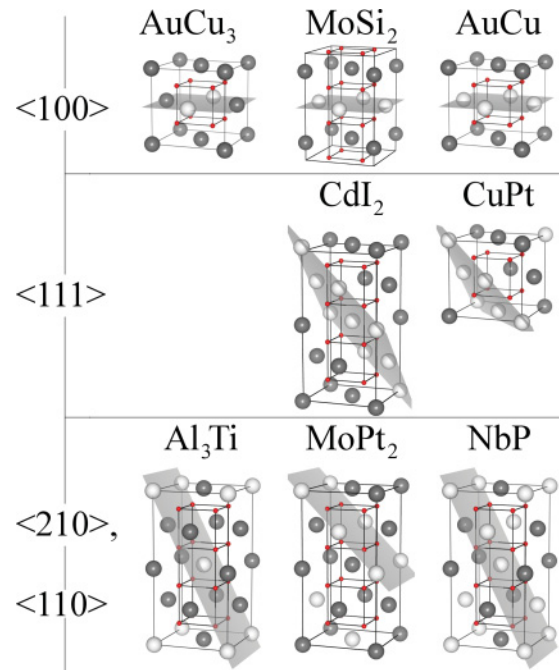

FIG. 1. (Color online) An illustration of the prototype ordered structures considered in the DFT + U calculations for the five compositions of mixed oxide explored. Ordering waves are identified and the stacking planes are shown in gray. The oxygen cubic sublattice is also shown.

TABLE I. Compositions, prototypes, Strukturbericht designation, and associated ordering wave families for the ordered structures considered in the DFT + U calculations.

Composition	Prototype	Strukturbericht	Ordering wave
A_3B	$AuCu_3$	$L1_2$	$\langle 100 \rangle$
A_2B	$MoSi_2$	$C11_b$	$\langle 100 \rangle$
A_2B_2	$AuCu$	$L1_0$	$\langle 100 \rangle$
A_2B	CdI_2	$C6$	$\langle 111 \rangle$
AB	$CuPt$	$L1_1$	$\langle 111 \rangle$
A_3B	Al_3Ti	$D0_{22}$	$\langle 210 \rangle$
A_2B	$MoPt_2$		$\langle 110 \rangle$
A_4B_4	NbP		$\langle 210 \rangle$

A. First-principles calculations

All DFT + U calculations have been performed employing the formalism of Dudarev *et al.*,[22] as implemented in the Vienna *ab initio* simulation package (VASP).[23–25] For this work, we have utilized the projector augmented-wave (PAW) method[26,27] and the Perdew-Burke-Ernzerhof generalized gradient approximation (PBE-GGA).[28,29] The PAW-PBE potentials employed in this work are those designated "U," "Ce," and "O" in the VASP library. The electronic wave functions were expanded in a plane-wave basis set with a cutoff of 500 eV, and the electronic states were sampled using k-point meshes centered on the origin, with a density equivalent to that of a $4 \times 4 \times 4$ mesh in the Brillouin zone of the ideal fluorite structure. The structures were fully relaxed with no symmetry constraints imposed, until the magnitude of the forces was below 10^{-3} eV/Å and the pressure was below 1 kBar. With these settings the calculated mixing energies are estimated to be converged to within 0.1 kJ per mole $(U,Ce)O_2$. The mixing enthalpy is defined as follows:

$$\Delta H_{\mathrm{mix}} = H_{U_{1-x}Ce_xO_2} - [(1-x)H_{UO_2} + x H_{CeO_2}], \quad (2)$$

where $H_{U_{1-x}Ce_xO_2}$ denotes the energy (per cation) of a urania-ceria mixture with x denoting the cation mole fraction of cerium ions, and similarly for H_{UO_2} and H_{CeO_2}. All of the results presented in this paper were calculated using the scalar-relativistic approximation. For the $L1_0$ ICS and MCS structures, we also performed calculations including spin-orbit coupling and the resulting mixing energies were found to change by a magnitude of less than 0.34 kJ/mol for the ICS and 2.41 kJ/mol for the MCS.

The differences in energy between MCS and ICS for a given structure are highly sensitive to the choice of values used for the parameter $U_{eff} = U-J$ in the DFT + U formalism employed in this work. The values of U_{eff} for U $5f$ and Ce $4f$ electrons utilized in the present calculations yield a close match between the calculated and experimental values of relevant oxidation and reduction energies. For uranium, the choice of $U_{eff} = 3.99$ eV, which was proposed originally by Dudarev *et al.*[22] and has been widely used in the literature, was found in the present study to give rise to good agreement between the calculated and measured values of the enthalpy changes for the following two oxidation reactions: (i) $UO_2 + \frac{1}{2} O_2 \rightarrow \gamma\text{-}UO_3$, (ii) $3\,UO_2 + O_2 \rightarrow \alpha\text{-}U_3O_8$. Descriptions of $\gamma\text{-}UO_3$ and the $\alpha\text{-}U_3O_8$ can be found in Refs. 30 and 31, respectively. With

$U_{eff} = 3.99$ eV, and employing the correction for overbinding of the oxygen molecule discussed in Ref. 32, we obtain values of $\Delta H_{rxn} = -1.45$ eV and -3.44 eV for reactions (i) and (ii), which agrees well with the corresponding experimental values of -1.44 and -3.31 eV, as determined from the Committee on Data for Science and Technology (CODATA) Key Values for Thermodynamics.[33] For cerium we choose the value $U_{eff} = 3$ eV, which was shown by Andersson *et al.*[34] to yield good agreement between calculated and experimental values for the enthalpy of the reduction reaction: $Ce_2O_3 + \frac{1}{2} O_2 \rightarrow 2\,CeO_2$. We note that in the context of the bond length distributions presented below, the combination of U_{eff} values and PBE exchange-correlation potential used in this work results in an overestimation of volumes for UO_2 and CeO_2 by 4.2% and 2%, respectively.

B. Electronic and ionic relaxation

An important issue that has been recently discussed in the literature[35–37] concerns the propensity for DFT + U calculations to converge to multiple self-consistent solutions corresponding to different orbital occupations. To ensure that such calculations converge to solutions that are the lowest-energy electronic states (or near them), several different methods have been proposed.[35–37] In the current work we employ the approach described by Meredig *et al.*,[37] which involves a slow localization of the f electrons in a series of DFT + U calculations with incrementally increasing values of U_{eff}. Specifically, one begins by performing a GGA (with $U_{eff} = 0$) calculation until ionic positions and charge density are converged. The wave functions, charge densities, and atomic positions are then used as the starting point for a calculation with a small nonzero value of U_{eff}, again performed to convergence of ionic position and charge density. The results of this calculation are then used as the starting point for a calculation with an incrementally higher U_{eff}, and this process is continued until the desired U_{eff} is reached. Steps in U_{eff} of approximately 0.1 eV have been found sufficient to reproducibly converge to the low-energy structure of UO_2.

For urania-ceria mixtures, this approach becomes somewhat ambiguous. Specifically, U_{eff} can be incremented for each ion-type simultaneously or in two separate stages. However, this ambiguity has been exploited in the current work to enable convergence of the electronic structure to the ICS and MCS charge configurations. Specifically, we find that the ICS charge state (i.e., composed of Ce^{4+} and U^{4+}) is obtained if U_{eff} is first ramped up to its final value on uranium $5f$ electrons, while holding the value of $U_{eff} = 0$ for the cerium $4f$ electrons. Alternatively, if U_{eff} is first applied to cerium $4f$ electrons, the MCS charge state (i.e., containing Ce^{3+} and U^{5+}) is obtained.

The oxidation states of the ions resulting from the calculations described above are identified based on three considerations: the interatomic bond lengths, the number of states in the occupied electronic partial densities of states, and the local magnetic moments. For structures with Ce^{3+} ions, the number of states in the occupied Ce $4f$ projected densities of states is found to integrate to approximately one electron (cf. Fig. 4), while this band lies above the Fermi level for structures containing only Ce^{4+} ions. Similarly, the number of states in the occupied U $5f$ projected densities of states is

approximately two and one for U^{4+} and U^{5+}, respectively. Corresponding to these different charge states are distinct values of the local magnetic moments. For U^{4+}, U^{5+}, Ce^{3+}, and Ce^{4+} ions the calculated local moments are close to the ideal values of 2, 1, 1, and 0, respectively, as expected from Hund's rule, which assumes that these moments originate from the single and paired f electrons. A final consistency check associated with the labeling of the charge states is made based on the calculated relaxed bond lengths. Oxidation of U^{4+} to U^{5+} is found to lead to the expected decrease in the average relaxed U-O bond lengths, while the reduction of Ce^{4+} to Ce^{3+} leads to an increase of the Ce-O bond lengths (cf. Fig. 3).

C. Classical pair potentials

To understand the implications of the DFT + U results for the finite-temperature thermodynamic properties of urania-ceria mixtures, we have used the DFT + U-calculated energies for ordered superstructures to refine previously published ionic pair-potential models for use in calculations of disordered solid solution energetics. The pair potentials are of the polarizable-shell model variety, and based on a Born-like description of the lattice, with long-range Coulombic interaction and short-range interactions that are accounted for via the Buckingham potential

$$E(r_{ij}) = \frac{q_i q_j}{r_{ij}} + A\exp\left(\frac{-r_{ij}}{\rho}\right) - \frac{C}{r_{ij}^6}, \qquad (3)$$

where q_i is the ionic charge, r_{ij} is the distance between particles i and j, and A, ρ, and C are adjustable parameters. In addition to the Buckingham short-range interactions, polarizabilities are introduced via intraatomic core-shell interactions, coupling Coulombic forces and a spring constant k, as per the formulation by Dick and Overhauser.[38] The Buckingham, charge, and spring-constant parameters are given in Refs. 17–20 for the O^{2-}, U^{4+}, Ce^{3+}, and Ce^{4+} ions, and are reproduced in Table II for reference. Also included in Table II are potential parameters for the U^{5+} ion developed by one of us previously.[39]

In applying these potentials to urania-ceria solid solutions with mixed charge states, an additional parameter is needed: uranium's fifth ionization energy minus cerium's fourth ionization energy. That is, for the reaction in Eq. (1) to proceed, an amount of energy corresponding to the combined ionization and binding of an electron on U^{4+} and Ce^{4+}, respectively, is required. Without knowing this energy difference, one cannot compare energetics between pair-potential calculations which have differing degrees of charge transfer. To maximize agreement with DFT + U results, and thereby treat pair-potential
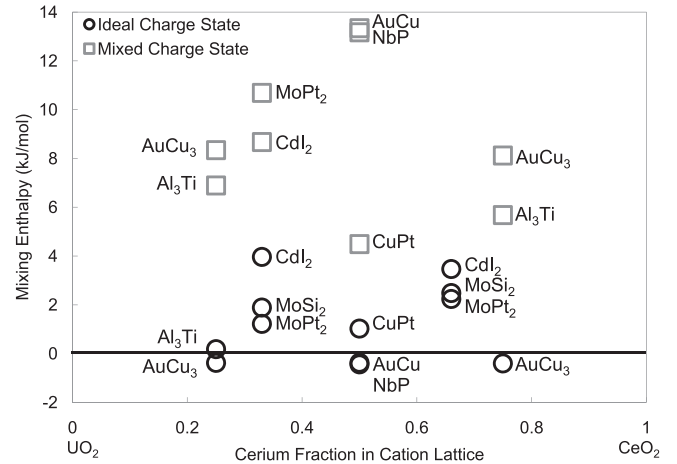

FIG. 2. Zero temperature mixing enthalpies for ordered structures shown in Fig. 1 as a function of Ce fraction on the cation sites. Energies for MCS compounds are shown with gray squares, while those for ICS compounds are indicated by black circles.

calculations as a suitable extension of those results, we use a value of 10.72 eV (or 1034 kJ per mole of electrons) for this combined ionization/binding energy, obtained by fitting to the DFT + U results. For this choice, the mixing energies of the ordered compounds at $x = 0.25$, 0.50, and 0.75, described above, agree within a standard deviation of 4.5 kJ/mol.

Using the pair-potential parameters described above, we computed the energetics of randomly disordered solid solutions with compositions up to $x = 0.25$. This range is chosen for two reasons: first, cerium as a fission product is dilute; and second, the cation fraction of plutonium (for which cerium is being treated as a surrogate) in high burnup MOX fuel is less than 0.20. Thus, the uranium-rich solid solutions are considered most relevant in the context of nuclear fuels. To compute solid solution energies we used supercells containing 256 cation sites randomly occupied by Ce^{4+} and U^{4+} for ICS models, and by U^{4+}, U^{5+}, Ce^{3+}, and Ce^{4+} for the various MCS states. We considered models with $x = 0.031$, 0.0625, 0125, 0.156, 0.219, and 0.25. For each composition we considered ICS states as well as two MCS states with 50% and 100% of the Ce ions reduced to the 3+ state (and a corresponding number of U ions oxidized to the 5+ state to maintain charge neutrality). At each of the resulting 18 compositions 300 supercells were generated with different random-number seeds. For each of the constructed supercells, full geometry relaxations were performed employing the GULP software.[40]

TABLE II. Buckingham and core-shell parameters employed in this work. Core-shell parameters (shell charge and spring constant) are applicable to the first ion identified in the "Interaction" column.

Reference	Interaction	A (eV)	ρ (Å)	C (eV Å^6)	Shell Charge Y(e)	Spring Const k (eV Å^{-2})
Binks *et al.*, 1993 (Ref. 20)	O^{2-}-O^{2-}	9547.960	0.219160	32.00	−2.04	6.3
Levy *et al.*, 2004 (Ref. 19)	Ce^{3+}-O^{2-}	2034.180	0.343800	15.86		
Vyas *et al.*, 1998 (Ref. 18)	Ce^{4+}-O^{2-}	1809.680	0.334700	20.40	−0.20	177.84
Busker *et al.*, 1999 (Ref. 17)	U^{4+}-O^{2-}	1761.775	0.356421		−0.10	160.00
Stanek and Grimes (Ref. 39)	U^{5+}-O^{2-}	2386.420	0.341100			

III. RESULTS

A. First-principles results

Figure 2 plots DFT $+ U$ calculated values of the mixing energies for each of the prototype ordered structures shown in Fig. 1 for both ICS and MCS states. Considering first the ICS structures, the mixing energies range from very weakly negative values with a magnitude less than 1 kJ/mol to positive values less than 5 kJ/mol. All of the MCS structures are calculated to be higher in energy than their corresponding ICS analogues at the same composition. However, the difference in energy between ICS and MCS states is seen to be sensitive to the nature of the cation ordering. For example, focusing on the structures at equiatomic composition, the AuCu and NbP structures, which are built from $\langle 100 \rangle$ and $\langle 1\frac{1}{2}0 \rangle$ special-point ordering waves, respectively, have energies that increase by 14 kJ/mol in going from the ICS to MCS states. By contrast, the CuPt structure, built from $\langle \frac{1}{2}\frac{1}{2}\frac{1}{2} \rangle$ ordering waves, is only 4 kJ/mol higher in energy in the MCS relative to the corresponding ICS state. A comparison of the results at each composition also shows an interesting trend that the structures with the highest energies in the ICS states have the lowest energies in the MCS states. In general, the variation in the energy differences between ICS and MCS states for the different structures suggests a significant coupling between the nature of the cation order and the energetics associated with charge transfer in the system.

In Fig. 3 we compile results for the calculated atomic structures of the ICS and MCS compounds. The results are plotted in the form of distributions of bond lengths between the different cation species and their eight nearest-neighbor oxygen ions. These distributions are derived from the fully relaxed structures of all the ICS and MCS compounds considered in the DFT $+ U$ calculations. For ICS ordering, the averaged lengths for U^{4+}-O and Ce^{4+}-O bonds are both 2.39 Å. In the MCS compounds, the U^{4+} and U^{5+} bond-length distributions overlap significantly, although the latter show a clearly smaller average bond length, as expected: The averaged values for the U^{4+}-O bond length in the MCS compounds is 2.40 Å, which is similar to its averaged value in the ICS structures, while the corresponding value for U^{5+}-O in the MCS compounds is 2.34 Å. The distribution of Ce-O bond

lengths in the MCS compounds is seen to be significantly narrower than that of the U-O bonds in the same structures. The average Ce^{4+}-O bond length in the MCS compounds has a value of 2.39 Å which is very similar to that in the ICS structures. The Ce^{3+}-O bond length is larger, as expected, with an average value in the MCS compounds of 2.46 Å. Overall, the results display the expected trends associated with changes in the cation radii with different oxidation states. The broader distributions for the U-O bond lengths in the MCS relative to the ICS compounds suggests a higher degree of strain energy in the former structures, with the preferred bond lengths for the different cation charge states being accommodated to differing degrees depending on the nature of the cation ordering.

The differences in the electronic structures for ICS versus MCS compounds is illustrated by the calculated electronic densities of states (DOS) for the equiatomic AuCu prototype structure in Fig. 4. In this figure, the ICS structure features a narrow band just below the Fermi level corresponding to the occupied $5f$ orbitals for the U^{4+} ions. This band is split off from the oxygen $2p$ band with a gap of 0.80 eV. In the MCS compound, the U $5f$ states shift to significantly lower energies with the highest density of states for these orbitals found at the edge of the O $2p$ band. The U^{5+}-O bonding thus displays a significantly stronger degree of covalent character, characterized by a stronger hybridization between the U $5f$ and O $2p$ states in the MCS compound. The occupied Ce $4f$ states for the Ce^{3+} ion in the MCS compound are observed to be split off from the U $5f$ and O $2p$ bands by a gap of approximately 2 eV, and these states display a much lower degree of hybridization with the O $2p$ orbitals.

B. Pair-potential modeling

The DFT $+ U$ results presented in Fig. 2 have been derived for long-range-ordered compounds featuring prototypical ordering of U and Ce ions on the fcc cation sublattice. As discussed above, urania-ceria mixtures observed experimentally are disordered solid solutions. To investigate the implications of the DFT $+ U$ results for the mixing thermodynamics of disordered solid solutions we have undertaken calculations based on classical ionic pair-potential models, as described in Sec. II C.
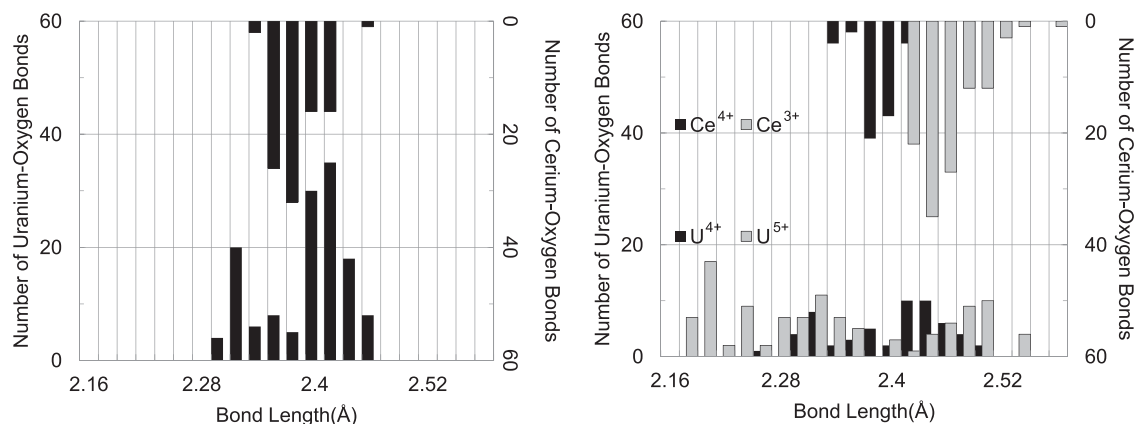

FIG. 3. Bond length distributions for ICS ordering (left panel) and MCS ordering (right panel). Distributions are summed over all structures considered in the DFT $+ U$ calculations, amounting to a total of 384 metal-oxygen bonds for the ICS and 352 for the MCS compounds.
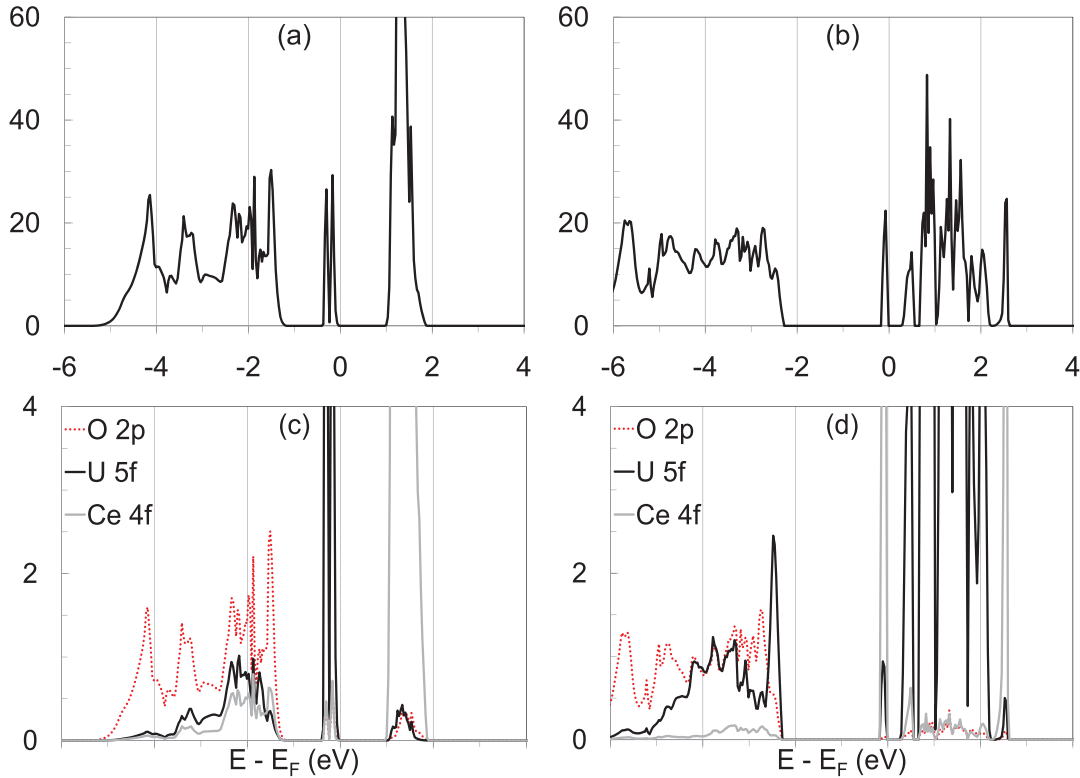
FIG. 4. (Color online) DFT + U calculated electronic density of states for a $(U_{0.5}Ce_{0.5})O_2$ compound with the AuCu-type cation ordering. The electronic DOS are plotted as a function of the energy relative to the Fermi energy E_F. Results for total DOS are plotted for (a) ICS and (b) MCS states. Oxygen $2p$, uranium $5f$, and cerium $4f$ partial densities of states are plotted for (c) ICS and (d) MCS states.

Figure 5 plots the averaged values (symbols) and standard deviations (error bars) of the mixing energies calculated
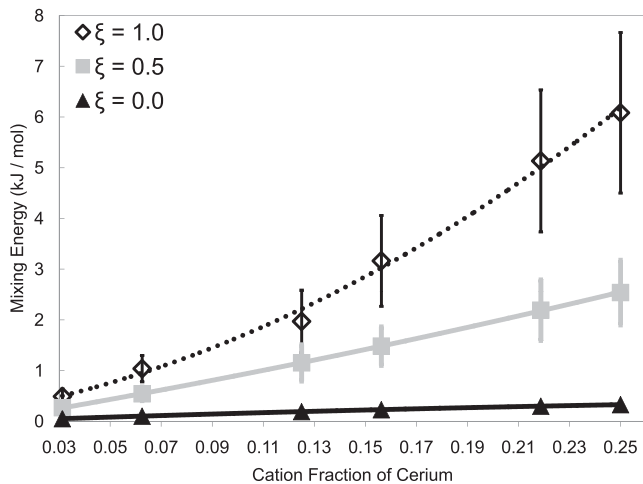

FIG. 5. Average mixing enthalpies obtained from ionic pair-potential calculations for structures generated by randomly arranging the cation sublattice of the fluorite structure. The average mixing energy obtained for each composition is given by a filled symbol and the solid lines are polynomial fits, included to highlight the trends. Error bars represent ± 1 standard deviation in all of the data for a given composition. "ξ" is the mole fraction of Ce which is in the Ce^{3+} state, as defined in the text.

by averaging over supercell configurations with randomly generated cation and charge disorder. The results are plotted for three different fractions of the degree of charge transfer, indicated by the value $\xi = x_{Ce^{3+}}/(x_{Ce^{3+}} + x_{Ce^{4+}})$, where $x_{Ce^{3+}}$ and $x_{Ce^{4+}}$ denote the cation mole fractions of Ce^{3+} and Ce^{4+} ions, respectively. The mixing energies for the ICS states ($\xi = 0$) are small and positive in magnitude, consistent with the DFT + U results for the ordered ICS structures in Fig. 2. With increasing degree of charge transfer, the mixing energy is seen to increase and is analogous to the DFT calculations, in which charge transfer is disfavored energetically. The increased variation in the energies of structures with high degrees of charge transfer is reflected by the larger standard deviations in the calculated mixing energies.

Although charge transfer is found to lead to a higher energy of the MCS relative to the ICS states in Figs. 2 and 5, this difference is relatively small, such that the MCS configurations are expected to be sampled for entropic reasons at the temperatures used in the synthesis and applications of urania-based fuels. To demonstrate this point, we show in Fig. 6 the mixing free energy derived at $T = 1500$ K, obtained by combining the calculated mixing enthalpies with a mixing entropy that accounts for the charge and cation configurations as well as orbital degeneracies. Specifically, we assume random cation and charge mixing so that the configurational entropy is approximated by the ideal-solution form, and we account for the degeneracy (W) of the lowest-energy f orbital states in a cubic crystal field. These are $W = 3$, 4, and 1
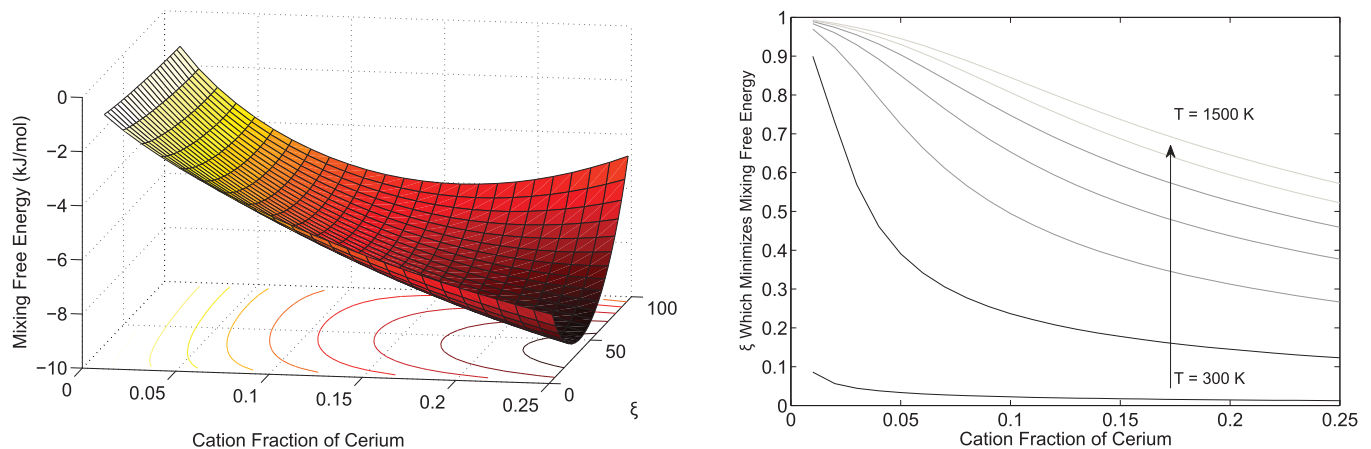
FIG. 6. (Color online) The left panel displays the ideal mixing free energy surface at 1500 K as a function of the two composition variables, cerium cation fraction ("x"), and the percentage of the Ce ions which are in a charge state of 3+ ("ξ"). The right panel displays how this approximation translates to the most favorable degree of charge transfer as a function of temperature.

for the f^2 (U^{4+}), f^1 (Ce^{3+} and U^{5+}), and f^0 (Ce^{4+}) states, respectively.[36,41,42] The resulting expression is

$$\Delta G_{\mathrm{mix}} = \Delta H_{\mathrm{mix}}(x_{\mathrm{Ce}^{3+}}, x_{\mathrm{Ce}^{4+}}, x_{\mathrm{U}^{4+}}, x_{\mathrm{U}^{5+}})$$
$$+ RT \left[\sum_i x_i \ln(x_i) \right] - RT x_{\mathrm{Ce}^{3+}} \ln\left(\frac{16}{3}\right), \quad (4)$$

with the mass and charge neutrality constraints

$$\sum_i x_i = x_{\mathrm{Ce}^{3+}} + x_{\mathrm{Ce}^{4+}} + x_{\mathrm{U}^{4+}} + x_{\mathrm{U}^{5+}} = 1, \quad (5)$$

$$3 x_{\mathrm{Ce}^{3+}} + 4 x_{\mathrm{Ce}^{4+}} + 4 x_{\mathrm{U}^{4+}} + 5 x_{\mathrm{U}^{5+}} = 4, \quad (6)$$

where x_i is the cation mole fraction for the given species with specified charge state. The assumptions underlying the formulation of this free energy are expected to be valid at relatively high temperatures, where random mixing is a reasonable assumption, but not too high such that the f electrons occupy excited states. The free energy is plotted as a function of the mole fraction of Ce and the fractional degree of charge transfer (ξ) in the left panel of Fig. 6. For a given Ce mole fraction the equilibrium value of ξ, which corresponds to the minimum in the free energy curve for a given Ce fraction, is seen to be non-zero. This figure thus illustrates that even though charge transfer is disfavored energetically, it is predicted to be stabilized within the lattice at nonzero temperatures due to its entropic contributions.

The right panel of Fig. 6 plots the composition and temperature dependence of the equilibrium value of ξ (i.e., the value which minimizes ΔG_{mix}). The results display an appreciable degree of charge transfer, particularly in dilute solutions at high temperatures. The equilibrium degree of charge transfer decreases with increasing Ce concentrations and/or decreasing temperature. This behavior reflects the fact that the degree of charge transfer is driven by entropic contributions to the free energy, and these contributions increase with increasing charge disorder. We note here that the entropic stabilization of mixed charge states, suggested in the present calculations for urania-ceria solid solutions, has also been shown in recent calculations for LiFePO$_4$ battery materials.[15]

In the next section we discuss the results in Fig. 6 in the context of experimental observations related to charge transfer in the urania-ceria system. While the free energy model given by Eq. (4) is based on estimates for the mixing enthalpy and the configurational entropy that are strictly valid only at high temperatures, the results in the right panel of Fig. 6 should hold even at low temperatures where the cation configurations are effectively frozen in by quenching from high temperature, and are immobile on the time scale of experimental measurements. Specifically, the total mixing entropy in Eq. (4) contains contributions from cation configurational disorder (i.e., irrespective of charge state) and electronic configurational degrees of freedom that arise from both charge mixing and orbital degeneracies. These two types of disorder can be shown to give independent additive contributions to the mixing entropy; removing the entropy associated with the cation configurational disorder (i.e., subtracting the contribution $-R[x ln(x) + (1 - x)ln(1 - x)]$) from the total mixing entropy leads to the contributions that are referred to as "electronic." These electronic contributions to the mixing entropy are the same whether the cations are considered frozen or their configurational entropy is accounted for. Thus, if a cation configuration is quenched to low temperatures where the cations are immobile (due to low diffusion rates), but charge disorder is still sampled (e.g., by a polaron hopping mechanism between neighboring U and Ce ions), the equilibrium values of ξ derived from Eq. (4) and plotted in the right panel of Fig. 6 remain unchanged.

IV. SUMMARY AND DISCUSSION

In this work we have examined computationally the mixing thermodynamic properties of (U$_{1-x}$Ce$_x$)O$_2$ using DFT + U calculations, classical pair-potential methods, and mean-field thermodynamic models. The mixing energies obtained by DFT + U calculations for prototypical fluorite-based, cation-ordered structures have a relatively small magnitude, on the order of 1–5 kJ/mol, when Ce and U take on the ideal 4+ charge state. With the values of the Hubbard U$_{\mathrm{eff}}$ parameter used in this work, DFT + U calculations predict

that charge transfer between U^{4+} and Ce^{4+} cations (resulting in the formation of U^{5+} and Ce^{3+}) leads to an increase in mixing energy by an amount that varies with the nature of the cation arrangement. We note that the sign and magnitude of the effect of charge transfer on the mixing energetics is sensitive to the choice of the U_{eff} parameters in the DFT $+ U$ method used in this work. The results presented here are based on values for U_{eff} that lead to a good match (accounting for overbinding of the oxygen molecule) between calculated and measured values of the energy for relevant reduction and oxidation reactions involving UO_2 and CeO_2.

Despite the predicted tendency for charge transfer to energetically destabilize urania-ceria solid solutions, the energy differences between ideal and mixed-charge states obtained in this work are small enough that charge mixing would be entropically stabilized at the high temperatures (e.g., 1500 K) relevant to both the synthesis of these materials, and applications of nuclear fuels. This point was illustrated in Sec. III B using a mixing free energy model based on values for ΔH_{mix} obtained by pair-potential models for random mixtures of U^{4+}, Ce^{4+}, U^{5+}, and Ce^{3+} cations, and a mixing entropy containing contributions from configurational ionic disorder, as well as electronic contributions associated with charge mixing and f orbital degeneracies. This free-energy model predicts an equilibrium degree of charge transfer, quantified by the variable $\xi = x_{Ce^{3+}}/(x_{Ce^{3+}} + x_{Ce^{4+}})$ that depends strongly on temperature and composition, as shown in the right panel of Fig. 6.

For concentrated mixtures at low temperatures, the results in Fig. 6 predict a very small degree of charge transfer. This result is not inconsistent with the conclusions drawn from room-temperature XANES measurements for $(U_{0.33}Ce_{0.67})O_2$ mixtures,[12] where an immeasurable concentration of Ce^{3+} was reported. From detailed measurements of Néel temperatures, low-temperature magnetic susceptibilities, and electron paramagnetic resonance (EPR), Hinatsu and Fujino concluded that charge transfer occurs to nonzero, albeit limited, extent in urania-ceria solid solutions even at the low temperatures where their measurements were conducted.[9–11] A detailed analysis of the magnetic properties of urania-ceria mixtures within the current model of charge transfer is beyond the scope of the current work. However, we note that EPR signals that were interpreted to result from the presence of U^{5+} ions were reported to be only measurable for Ce cation mole fractions below 0.1 in Ref. 11. A larger number of U^{5+} ions for low Ce concentrations is consistent with the sharply rising values of ξ at dilute compositions shown in Fig. 6. Finally, concerning the XPS data of Bera *et al.*,[13] we note that charge transfer was shown in Fig. 2 to be associated with pronounced lattice distortions. Given this, the equilibrium degree of charge disordering could be significantly enhanced near the surface relative to the bulk, as the strain energy would presumably be more easily accommodated near a free surface. Such effects are a possible reason for the enhanced degree of charge transfer derived from the analysis of the XPS data, relative to that obtained in the XANES studies.

The increase in the degree of charge transfer (ξ) with the temperature shown in Fig. 6 implies that the electronic contribution to the mixing entropy (ΔS_{mix}) will also increase with increasing T, leading to a positive value for the excess heat capacity $\Delta C_P = T(\partial \Delta S_{mix}/\partial T)_P$. Measurements of C_P for UO_2, CeO_2, and $(U_{1-x}Ce_x)O_2$ mixtures (with $x = 0.2$, 0.5, and 0.8) were performed most recently by Krishnan and Nagarajan[8] from room temperature to 800 K, and these results do indeed show a significant positive excess heat capacity. Over this temperature range, cation configurational degrees of freedom associated with diffusion are not expected to be sampled on the time scale of the experiments, so that the positive ΔC_P values would reflect electronic contributions to ΔS_{mix} that increase with T, as described at the end of Sec. III B. In contrast to these results, however, heat capacities for $(U_{0.9}Ce_{0.1})O_2$ solid solutions measured by Arita[7] give rise to negative values of ΔC_P when compared to published C_P data for CeO_2 and UO_2. Further work is warranted to elucidate the origin of these discrepancies in the heat-capacity data, as the quantity ΔC_P provides important insights into the nature of the nonconfigurational contributions to the mixing thermodynamic properties in this system.

Overall, the results obtained in this work suggest that the long-standing question concerning the degree of charge transfer in urania-ceria solid solutions is one that should be discussed with reference to sample composition, temperature, and thermal history. Further understanding of this issue would clearly benefit from expanded theoretical and experimental work. Computationally, a more accurate free-energy model is needed that relaxes the assumptions of random mixing, and alternate electronic-structure methods for correlated electrons would be worth investigating to check the robustness of the DFT $+ U$ results. Experimentally, multiple measurements probing both thermochemical and spectroscopic properties on the same set of samples at varying temperatures and composition would be particularly useful.

[1] T. Markin, R. Street, and E. Crouch, J. Inorg. Nucl. Chem. **32**, 59 (1970).

[2] R. Lorenzelli and B. Touzelin, J. Nucl. Mater. **95**, 290 (1980).

[3] A. Murray, C. Catlow, and B. Fender, J. Chem. Soc., Faraday Trans. 2 **83**, 1113 (1987).

[4] T. Lindemer and J. Brynestad, J. Am. Ceram. Soc. **69**, 867 (1986).

[5] K. Yamada, S. Yamanaka, T. Nakagawa, M. Uno, and M. Katsura, J. Nucl. Mater. **247**, 289 (1997).

[6] P. Martin, M. Ripert, T. Petit, T. Reich, C. Hennig, F. D'Acapito, J. Hazemann, and O. Proux, J. Nucl. Mater. **312**, 103 (2003).

[7] Y. Arita, T. Matsui, and S. Hamada, Thermochim. Acta **253**, 1 (1995).

[8] R. Krishnan and K. Nagarajan, Thermochim. Acta **440**, 141 (2006).

[9] Y. Hinatsu and T. Fujino, J. Solid State Chem. **73**, 348 (1988).

[10] Y. Hinatsu and T. Fujino, J. Less-Common Met. **149**, 197 (1989).

[11] Y. Hinatsu and T. Fujino, Chem. Phys. Lett. **172**, 131 (1990).

[12] M. Antonio, U. Staub, J. Xue, and L. Soderholm, Chem. Mater. **8**, 2673 (1996).

[13] S. Bera, V. K. Mittal, R. V. Krishnan, T. Saravanan, S. Velmurugan, K. Nagarajan, and S. V. Narasimhan, J. Nucl. Mater. **393**, 120 (2009).

[14] T. Griffiths, H. Hubbard, and M. Davies, Inorg. Chim. Acta **225**, 305 (1994).

[15] F. Zhou, T. Maxisch, and G. Ceder, Phys. Rev. Lett. **97**, 155704 (2006).

[16] S. Dudarev, G. Botton, S. Savrasov, Z. Szotek, W. Temmerman, and A. Sutton, Phys. Status Solidi A **166**, 429 (1998).

[17] G. Busker, A. Chroneos, R. Grimes, and I. Chen, J. Am. Ceram. Soc. **82**, 1553 (1999).

[18] S. Vyas, R. Grimes, D. Gay, and A. Rohl, J. Chem. Soc., Faraday Trans. **94**, 427 (1998).

[19] M. Levy, R. Grimes, and K. Sickafus, Philos. Mag. **84**, 533 (2004).

[20] D. Binks and R. Grimes, J. Am. Ceram. Soc. **76**, 2370 (1993).

[21] F. Ducastelle, *Order and Phase Stability in Alloys (Cohesion and Structure)* (North Holland, Amsterdam, 1991).

[22] S. L. Dudarev, G. A. Botton, S. Y. Savrasov, C. J. Humphreys, and A. P. Sutton, Phys. Rev. B **57**, 1505 (1998).

[23] G. Kresse and J. Hafner, Phys. Rev. B **47**, 558 (1993).

[24] G. Kresse and J. Furthmuller, Phys. Rev. B **54**, 11169 (1996).

[25] G. Kresse and J. Furthmuller, Comput. Mater. Sci. **6**, 15 (1996).

[26] P. E. Blochl, Phys. Rev. B **50**, 17953 (1994).

[27] G. Kresse and D. Joubert, Phys. Rev. B **59**, 1758 (1999).

[28] J. P. Perdew, K. Burke, and M. Ernzerhof, Phys. Rev. Lett. **77**, 3865 (1996).

[29] J. Perdew, K. Burke, and M. Ernzerhof, Phys. Rev. Lett. **78**, 1396 (1997).

[30] R. Engmann and P. Wolff, Acta Crystallogr. **16**, 993 (1963).

[31] B. Loopstra, Acta Crystallogr. **17**, 651 (1964).

[32] L. Wang, T. Maxisch, and G. Ceder, Phys. Rev. B **73**, 195107 (2006).

[33] J. Cox, D. Wagman, and V. Medvedev, *CODATA Key Values for Thermodynamics* (Hemisphere Publishing Corp., New York, 1984).

[34] D. A. Andersson, S. I. Simak, B. Johansson, I. A. Abrikosov, and N. V. Skorodumova, Phys. Rev. B **75**, 035109 (2007).

[35] B. Dorado, B. Amadon, M. Freyss, and M. Bertolus, Phys. Rev. B **79**, 235125 (2009).

[36] F. Zhou and V. Ozolins, Phys. Rev. B **80**, 125127 (2009).

[37] B. Meredig, A. Thompson, H. A. Hansen, C. Wolverton, and A. van de Walle, Phys. Rev. B **82**, 195128 (2010).

[38] B. Dick and A. Overhauser, Phys. Rev. **112**, 90 (1958).

[39] C. Stanek, A. Cleave, and R. Grimes, (unpublished).

[40] J. Gale and A. Rohl, Mol. Simul. **29**, 291 (2003).

[41] F. Zhou and V. Ozolins, Phys. Rev. B **83**, 085106 (2011).

[42] F. Zhou, private communication.